Preclinical Pharmacology and Pharmacokinetics of AZD3783, a Selective 5-HT$_{1B}$ Receptor Antagonist

Minli Zhang, Diansong Zhou, Yi Wang, Donna L. Maier, Daniel V. Widzowski, Cynthia D. Sobotka-Briner, Becky J. Brockel, William M. Potts, Ashok B. Shenvi, Peter R. Bernstein and M. Edward Pierson

AstraZeneca Pharmaceuticals, 1800 Concord Pike, Wilmington, DE 19805

Departments of Drug Metabolism and Pharmacokinetics (M.Z., D.Z., Y.W., W.M.P.), Neuroscience (D.L.M., D.V.W., C.D.S., B.J.B.), Chemistry (A.B.S., P.R.B., M.E.P.), AstraZeneca Pharmaceuticals, Wilmington, DE, USA.

1

Running Title:

Preclinical Pharmacology of 5-HT$_{1B}$ Antagonist AZD3783

Corresponding author:

Minli Zhang, Ph.D.

Drug Metabolism and Pharmacokinetics

AstraZeneca Pharmaceuticals

35 Gatehouse Drive

Waltham, MA, USA 02451

Tel 1-781-839-4411

Fax 1-781-472-5926

Email minli.zhang@AstraZeneca.com

Number of Text pages: 28

Number of Tables: 5

Number of Figures: 9

Number of references: 38

Number of words in abstract: 247

Number of words in introduction: 741

Number of words in discussion: 913

ABBREVIATIONS:

5-HT, serotonin, 5-hydroxytryptamine; 5-HT$_{1B}$, serotonin 1B receptor; SSRIs, selective serotonin reuptake inhibitors; GPCR, G protein-coupled receptor; SNRI, serotonin norepinephrine reuptake inhibitors; CHO, Chinese hamster ovary cells; CTX, cortex; STR, striatum/globus pallidus ; MID, midbrain including substantia nigra; CRB, the cerebellum; PET, Positron Emission Tomography; CYP, cytochrome P450; MDR1-MDCK, Madin-Darby Canine Kidney cells transfected with human MDR1 gene; Pgp, P-glycoprotein; HLM, human liver microsome; RLM, rat liver microsome; DMEM, Dulbecco's modified Eagle's medium; LC-MS, liquid chromatography mass spectroscopy; MRM, Multiple Reaction Monitoring; PK, pharmacokinetics; CL$_{int}$, intrinsic clearance; CL, total plasma clearance; Vd, volume of distribution; Vd$_{ss}$, steady state volume of distribution; T$_{max}$, time to reach plasma maximum concentration; C$_{max}$, maximum plasma concentration; C$_{min}$, minimum plasma concentration; AUC, area under the curve; t$_{1/2}$, half-live; f$_u$, fraction unbound; IVIVC, *in vitro-in vivo* correlation; SPA, Scintillation Proximity Assay; GR125743, *N*-[4-methoxy-3-(4-*methyl*piperazin-1-yl)phenyl]-3-*methyl*-4-(4-pyridyl)benzamide; [*N-methyl*-^{3}H$_3$]AZ10419369, 5-*methyl*-8-(4-*methyl*-piperazin-1-yl)-4-oxo-4*H*-chromene-2-carboxylicacid (4-morpholin-4-yl-phenyl)-amide; AZD1134, 6-fluoro-8-(4-*methyl*-piperazin-1-yl)-4-oxo-4*H*-chromene-2-carboxylic acid [4-(4-propionyl-piperazin-1-yl)-phenyl]-amide; GTPγ^{35}S, guanosine 5γ-3-*O*-[^{35}S]triphosphate; CP135.807, 3-(*N*-methylpyrrolidin-2*R*-ylmethyl)-5-(3-nitropyrid-2-ylamino)-l*H*-indole; fmol/mg, femtomole per milligram.

Section assignment:

Neuropharmacology

ABSTRACT:

The preclinical pharmacology and pharmacokinetic properties of AZD3783, a potent 5-hydroxytryptamine 1B (5-HT$_{1B}$) receptor antagonist, were characterized as part of translational pharmacokinetic/pharmacodynamic hypothesis testing in human clinical trials. The affinity of AZD3783 to the 5-HT$_{1B}$ receptor was measured *in vitro* using membrane preparations containing recombinant human or guinea pig 5-HT$_{1B}$ receptors and in native guinea pig brain tissue. *In vivo* antagonist potency of AZD3783 for the 5HT$_{1B}$ receptor was investigated by measuring the blockade of 5-HT$_{1B}$ agonist-induced guinea pig hypothermia. The anxiolytic-like potency was assessed using the suppression of separation-induced vocalization in guinea pig pups. The affinity of AZD3783 for human and guinea pig 5-HT$_{1B}$ receptor (K$_i$ = 12.5 and 11.1 nM, respectively) was similar to unbound plasma EC$_{50}$ values for guinea pig receptor occupancy (11 nM) and reduction of agonist-induced-hypothermia (18 nM) in guinea pig. Active doses of AZD3783 in the hypothermia assay were similar to doses that reduced separation-induced vocalization in guinea pig pups. AZD3783 demonstrated favorable pharmacokinetic properties. The predicted pharmacokinetic parameters (CL = 6.5 mL/min/kg; Vd$_{ss}$ = 6.4 L/kg) were within 2-fold of the values observed in healthy male volunteers following a 20 mg single oral dose. This investigation presents a direct link between AZD3783 *in vitro* affinity and *in vivo* receptor occupancy to preclinical disease model efficacy. Together with predicted human pharmacokinetic properties, we have provided a model for the quantitative translational pharmacology of AZD3783 that increases confidence in the optimal human receptor occupancy required for antidepressant and anxiolytic effects in patients.

INTRODUCTION:

Serotonin or 5-hydroxytryptamine (5-HT) is a neurotransmitter in the central nervous system involved in physiological functions including thermoregulation, modulation of neuronal transmitter release, as well as anxiety and mood regulation (Delgado et al., 1990; Keane and Soubrié, 1997; Fink and Göther, 2007). Complex mechanisms have been proposed for the regulation of 5-HT levels in serotonergic synapses and terminal fields, such as release of 5-HT by serotonergic neurons, uptake of 5-HT through serotonin reuptake transporters and metabolism of 5-HT by monoamine oxidase (Möller and Volz, 1996). These mechanisms have been successfully exploited in developing numerous anxiolytics and antidepressants that increase 5-HT levels.

Currently, the selective serotonin, and serotonin/norepinephrine reuptake inhibitors (SSRIs and SNRIs) are first-line agents for treatment of anxiety and depression (Mendlewicz and Lecrubier, 2000; Nutt, 2008). However, therapy with SSRIs or SNRIs requires daily administration over the course of weeks for anxiolytic or antidepressant efficacy to emerge and it is often accompanied by the appearance of sedation, weight gain, nervousness, and a high incidence of sexual dysfunction (Goldstein and Goodnick, 1998; Sussman, 2008). Increased risk of suicidal ideation in children and adolescents treated with SSRIs has also received attention although conflicting findings have been reported (reviewed by Hetrick et al., 2010). Despite the success of SSRI therapies, up to 40% of major depressive disorder patients do not respond (Tsai and Honga, 2003), and patient's depressive symptoms often return during maintenance therapy (Byrne and Rothschild, 1998). This combined with the SSRI side-effect profiles and the slow onset of SSRI-mediated antidepressant effect, drive a significant demand for improved efficacy and tolerability in the treatment of anxiety and depression.

The pre-synaptic 5-HT$_{1B}$ autoreceptor also regulates 5-HT release, therefore, it has been considered as an alternative target to 5-HT reuptake transporters for antidepressants (Gaster et al., 1998; Hillegaart and Ahlenius, 1998; Roberts et al., 2001; Ahlgren et al., 2004; Dawson et al., 2006). This mechanism also has the potential to provide a rapid onset of clinical efficacy without the liabilities associated with SSRIs (Moret and Briley, 2000; Slassi, 2002). Animal models such as serotonin agonist-induced guinea pig hypothermia (Maj et al., 1988) and guinea pig pup separation-induced vocalization (Dawson et al., 2006; Hagan et al., 1997; Hudzik et al., 2003; Stenfors et al., 2004) were developed to screen and evaluate the pharmacology of serotonergic agents such as 5-HT$_{1B}$ receptor antagonists. Selective 5-HT$_{1B}$ antagonists such as AR-A000002 (Hudzik et al., 2003) and SB-616234-A (Dawson et al., 2006) have been shown to elevate serotonergic neurotransmission *in vivo* and exhibit effects indicative of antidepressant and anxiolytic properties in animals. The recent discovery of selective, high affinity 5-HT$_{1B}$ compounds made it possible to develop 5-HT$_{1B}$ specific ligands for Positron Emission Tomography (PET) to obtain non-invasive quantification of specific binding to the receptor in brain (Pierson et al., 2008; Nabulsi et al., 2010). These tools can provide an understanding of the level of receptor occupancy required for minimal and maximal efficacy and the margin to on-target side effects that is critical for formulating a testable translational pharmacology hypothesis for early human testing. For G protein-coupled receptor (GPCR) antagonists, such as 5HT$_{1A}$, 5-HT$_{2A}$ and NK1 antagonists, 50-87% receptor occupancy was required for therapeutic responses (Grimwood and Hartig, 2009). However, the optimal range of 5-HT$_{1B}$ receptor occupancy in brain by selective 5-HT$_{1B}$ antagonists that is required for antidepressant and anxiolytic efficacy in preclinical models and in patients has yet to be established.

Many properties, such as receptor affinity, functional antagonism, physicochemical properties, metabolic stability and efflux transporter substrate liabilities, will impact the doses and exposures needed to achieve efficacy in preclinical and clinical studies. An ideal 5-HT$_{1B}$ antagonist drug would possess pharmacodynamic and pharmacokinetic properties that enable it to occupy and block the 5-HT$_{1B}$ receptor at levels sufficient for antidepressant and anxiolytic efficacy following once daily dosing. AZD3783 (Figure 1), (2R)-6-methoxy-8-(4-methylpiperazin-1-yl)-N-(4-morpholin-4-ylphenyl)chromane-2-carboxamide, is a potent, selective 5-HT$_{1B}$ antagonist which was selected for further study because of its favorable pharmacological and pharmacokinetic profiles. In a recent report on PET studies using a 5-HT$_{1B}$ specific ligand, Varnäs et al. (2011) demonstrated specific and high affinity binding of AZD3783 to 5-HT$_{1B}$ receptors in human and non-human primate brains. The objective of this study was to characterize the *in vitro* and preclinical *in vivo* pharmacodynamic and pharmacokinetic properties of AZD3783 in order to develop a preclinical translational approach that would enable comparison with PET occupancy results in humans and help guide dose selection for the 5-HT$_{1B}$ antagonist in clinical hypothesis testing for anxiety and mood disorders.

MATERIALS AND METHODS

Materials. AZD3783, AZD1134 and radiolabeled ligand [*N*- methyl-$^3H_3$]AZ10419369 were synthesized at AstraZeneca Pharmaceuticals LP. [^3H]-GR125743 a 5-HT$_{1B}$ radiolabeled ligand was purchased from GE Healthcare (Chalfont St. Giles, Buckinghamshire, UK). Cryopreserved hepatocytes from human, male cynomolgus monkey, male Beagle dog and pooled cynomolgus monkey liver microsomes were purchased from CellzDirect (Durham, NC). Pooled human liver microsomes were obtained from BD Gentest (Woburn, MA). Fresh hepatocytes from male Sprague Dawley rats, liver microsomes from Sprague Dawley rats and Beagle dog were prepared within AstraZeneca using standard procedures. Plasma from rat, dog, cynomolgus monkey, guinea pig and human were obtained from Bioreclamation (Hicksville, NY). The 5-HT$_{1B}$ agonist, CP135.807 and other chemicals were purchased from Sigma-Aldrich (St. Louis, MO). The Madin-Darby Canine Kidney cell line transfected with human MDR1 (MDR1-MDCK) was obtained from The Netherlands Cancer Institute (Amsterdam, Netherlands). Dulbecco's modified Eagle's medium (DMEM) and fetal bovine serum were obtained from Invitrogen (Carlsbad, CA). The Chinese hamster ovary (CHO) cells expressing 5-HT$_{1B}$ receptors (10 mg/mL), reagents for the 5-HT$_{1B}$ assays, the OptiPlates, Soluene 350 and Ultima-Gold scintillation fluid were from PerkinElmer (Waltham, MA).

Animals. Husbandry, experimental use and methods of euthanasia met ethical guidelines for the humane care and treatment of laboratory animals. Male Sprague Dawley rats and Dunkin-Hartley guinea pigs were purchased from Charles River (Malvern, PA). The body weight of Sprague Dawley rats, Hartley guinea pigs, Beagle dogs and cynomolgus monkeys (*Macaca fascicularis*) ranged from 0.30-0.35 kg, 0.2-0.4 kg, 10-13 kg, and 3-8 kg, respectively. Except for guinea pigs in behavior studies, all the animals were fasted overnight before dosing

8

and were fed 2 hours after dosing. All animals were individually housed with free access to

water and maintained in rooms with constant temperature (approximately 22 °C) and a 12 hour

light/dark cycle. All facilities were approved by the American Association for Accreditation of

Laboratory Animal Care (AAALAC) and all testing procedures were performed using protocols

approved by the Institutional Animal Care and Use Committee at AstraZeneca R&D

Wilmington, in accordance with *The Guide for the Care and Use of Laboratory Animals*.

Pharmacology

In vitro pharmacology assays. The 5-HT$_{1B}$ receptor binding and GTPγ^{35}S functional

antagonist assays were modified from previously published procedures (Watson et al., 1996). In

the 5-HT$_{1B}$ receptor competition binding assays, a predefined quantity of membranes containing

human or guinea pig 5-HT$_{1B}$ receptors were diluted in assay buffer containing 50 mM Tris-HCl

(pH 7.4), 4 mM MgCl$_2$, 4 mM CaCl$_2$, 1 mM EDTA. The membranes in the 96-well OptiPlates at

10 µg/well were incubated with 0.5 nM of [^{3}H]-GR125743 and AZD3783 at concentrations from

170 pM to 10 µM. AZD1134, a potent and very selective 5HT$_{1B}$ antagonist synthesized at

AstraZeneca, was used to define non-specific binding at 1µM final assay concentration. The

pharmacology of AZD1134 was well-defined and it demonstrated structurally diversity from

AZD3783 (Maier et al., 2009). The assay plates were incubated for 1 hour at room temperature

with shaking. Amersham RPNQ0011 Yttrium Silicate-WGA SPA Beads (Amersham,

Piscataway, NJ) were then added to the plates at 1.5 mg/well and incubated for additional 30 min

with vigorous shaking. Following the incubation and centrifugation the radioactivity in each

well was measured in a TopCount scintillation counter (PerkinElmer, Waltham, MA).

In the GTPγ^{35}S functional antagonist scintillation proximity assay (SPA) assay,

membranes and compound dilutions were the same as those in 5-HT$_{1B}$ receptor binding assay. In

this SPA assay, membranes (15 µg protein/well), and Amersham RPNQ000 WGA PVT beads

(50 µg/well) (Amersham Piscataway, NJ) were pre-incubated in bulk in assay buffer containing

20 mM HEPES (pH 7.4), 100 mM NaCl, 10 mM MgCl$_2$, 0.1% BSA, for 30 min. After adding

GTPγ^{35}S (200 pM final assay concentration) and GDP (10 µM final) to the membrane/bead

mixture, 150 µl of the mixture was added to 96-well OptiPlates (PerkinElmer) containing 2 µl of

AZD3783 (170 pM to 10 µM at final concentration). After 5 min preincubation, 50 µl of buffer

or 108 nM 5-HT (27 nM final assay concentration at EC$_{80}$) were added. The plates were

incubated for 1 hour with shaking. Following centrifugation the radioactivity in each well was

measured in a TopCount. Percent effect with respect to basal (buffer unstimulated) and

stimulated (EC$_{80}$ of 5-HT) response was determined.

Guinea pig receptor binding assay. The guinea pig receptor occupancy assay was

conducted using methods reported by Maier et al. (2009). One to two days prior to the receptor

occupancy experiment, the jugular cannula was inserted for i.v. dosing. After the guinea pig was

anesthetized with isoflurane, a 2-3 French catheter was inserted into the jugular vein and

terminated at the right atrium. The exterior end of the cannula was fed subcutaneously, anchored

to the skin dorsal to the shoulder blades and flushed with 0.9% saline with 100 units/mL heparin

to test patency. On the day of the experiment, AZD3783 (0.06, 0.2, 0.6, 2.0, 6.0, 20.0 µmol/kg,

s.c.) or vehicle treatment (0.9% saline; volume 1mL/kg, s.c.) was administered to fed animals 30

min prior to [*N*-methyl-^{3}H$_3$]AZ10419369 (15 µCi/ml/guinea pig, i.v.). Guinea pigs were

euthanized 30 min after radioligand injection. Trunk blood samples were collected and plasma

was analyzed LC-MS to determine the plasma concentration of AZD3783. The brain was

removed and placed on a chilled plate for free-hand dissection into selected brain regions, including the cortex (CTX), striatum/globus pallidus (STR), midbrain including substantia nigra (MID) and the cerebellum (CRB). Each tissue region was frozen, weighed and transferred to scintillation vials containing Soluene 350. After solubilizing the tissue overnight, Ultima-Gold scintillation fluid was added and total radioactivity was measured using a Tri-Carb scintillation counter (Perkin Elmer, Waltham, MA). [N-methyl-$^3H_3$]AZ10419369 binding was determined for all treatment groups and presented as fmol/mg tissue.

Blockade of agonist-induced hypothermia in guinea pigs. This experiment was carried out over two days. On each day of the experiment, animals to be used were habituated to the test room for at least 1 hour before testing. Body weight and baseline rectal body temperatures were determined for each animal and then all subjects were assigned to one of nine treatment groups (N=6 per treatment group): vehicle + 3 mg/kg agonist (CP135.807); AZD 3783 at 0.006, 0.002, 0.06, 0.2, 0.6, 2, 6, or 20 μmol/kg + agonist. Depending on the treatment group, AZD3783 or vehicle was administered by s.c. injection 30 min prior to the administration of 5-HT$_{1B}$ agonist (3 mg/kg, i.p.). Previous experiments with CP135.807 (data not presented) had shown that this dose of this 5-HT$_{1B}$ agonist would induce approximately a two to three degree centigrade reduction in rectal temperature that lasted for several hours and that was sensitive to blockade by selective 5-HT$_{1B}$ antagonists. One hour after agonist administration, rectal body temperature was measured again. After body temperature measurement, each animal was quickly euthanized to obtain plasma and brain samples. The plasma and brain samples collected were rapidly frozen until analysis. Data were reported as body temperature (°C) and plasma or brain concentration.

Suppression of maternal separation-induced vocalizations in guinea pig pups. The testing apparatus was comprised of a blue tinted but see through, rectangular Rubbermaid storage

11

container 24.3"H × 16"W × 15.8"D. Audio recordings were made using a Sony BM-575

Microcassette Dictator and Sony 60 min micro cassettes. Testing of the pups was done in a

repeated measures design starting at 4 to 6 days postnatal and continued until 23 to 25 days

postnatal with at least 2 days between test days. The litters were transported to the testing lab

and allowed to acclimate for 1 hour prior to testing. All subjects were given a 5 min (300

seconds) pre-screen to measure the response to maternal separation by recording the number of

vocalizations emitted by each subject. After prescreening, four groups, each with 12 pups, were

dosed subcutaneously (1mL/kg) at 0 (vehicle), 0.2, 0.6, and 2.0 µmol/kg of AZD3783,

respectively. The dose vehicle contained sterile water with 85% lactic acid, pH 4.0. Following

the post-injection period, number of vocalizations emitted by each subject was assessed in a 5

min test session.

Pharmacokinetics (PK)

P-glycoprotein (Pgp) transporter assay. Monolayer-based Pgp assays were performed

manually in basolateral to apical (B→A) and apical to basolateral (A→B) directions in triplicate

(Polli et al., 2001). The MDR1-MDCK cells were seeded onto 12-well Costar Transwell plate

(Lowell, MA) at a density of 3×10^5 cells/cm^2 and grown in DMEM with 10% fetal bovine serum

for 3 days. The medium was replaced daily and at 2 hours before transport experiments. The

transport of AZD3783 was assessed at initial concentration of 1 µM for 60 min at 37 °C. At the

end of the experiment, samples from both donor and receiver chambers were analyzed by LC-

MS. The apparent permeability values were calculated with equation $P_{app} = 1/(A \times C_0) \times (dQ/dt)$,

where A is insert surface area, C_0 is initial donor drug concentration and dQ/dt is amount of drug

transported within a given time period. The flux ratio was calculated from $P_{app\ B \to A}$ divided by

$P_{app\ A \to B}$.

Plasma protein binding. Plasma protein binding of AZD3783 was determined by

equilibrium dialysis in a Spectrum equilibrium dialyzer using dialysis membranes with a 12,000

to 14,000-Da molecular mass cutoff (Rancho Dominguez, CA) against Dulbecco's phosphate

buffered saline (pH 7.4). Aliquots of 2 mL plasma were spiked with AZD3783 to achieve final

concentrations of 0.1, 1, and 10 μM with DMSO <0.5% in plasma. The dialysis was conducted

in triplicate for overnight at 37 °C. At the end of dialysis, aliquots of 100 μL plasma samples

were mixed with equal volume of buffer; aliquots of 100 μL buffer dialysate samples were mixed

with equal volume of plasma. Two volumes of acetonitrile containing 0.2% formic acid were

then added to these samples. After centrifugation for 15 min at 3000 rpm, the supernatant was

quantified by LC-MS. The unbound fraction (f_u) was calculated as the concentration of

AZD3783 in buffer divided by the concentration in plasma.

Microsome metabolic stability assay. In microsome stability assay, duplicate samples of

AZD3783 (1 μM) were incubated at 37 °C with liver microsomes (0.5 mg/ml) from human, rat,

dog or cynomolgus monkey, in 0.1 M potassium phosphate buffer (pH 7.4). NADPH (1 mM)

was added to initiate the incubation. Aliquots of the incubates were removed at 0, 5, 10, 15, 20

and 25 min, respectively, and added to equal volume of acetonitrile/methanol (1:1, v/v)

containing 0.1% formic acid to stop the reaction. After centrifugation for 10 min at 3500 rpm,

the remaining AZD3783 in the supernatant was analyzed by LC-MS.

Hepatocytes metabolic stability assay. The hepatocyte metabolic stability of AZD3783

was determined in duplicate at 1 μM with freshly isolated rat hepatocytes, or using

cryopreserved dog, monkey or human hepatocytes from three individual donors at 1×10^6

13

cells/mL. The incubation was carried out at 37°C in Williams E medium (pH 7.4), with 1%

GIBCO insulin transferrin selenium solution, 2 mM of *L*-glutamine and 25 mM of HEPES.

Aliquots of suspension were removed at 0, 5, 10, 15, 20, 25 and 30 min, respectively, and added

to equal volume of ice cold acetonitrile to stop the reaction. Following a 5 min centrifugation at

3500 rpm, the remaining AZD3783 in the supernatant was quantified by LC-MS.

Rat PK. The 5 mM AZD3783 solution was prepared in 25 mM lactic acid containing

3.75% Dextrose. The i.v. injection was introduced via tail vein at a dose of 10 µmol/kg. The

oral dose was administered by oral gavage at a volume of 6 mL/kg to achieve a target dose of 30

µmol/kg. Aliquots (0.15 mL) of blood samples were collected from the implanted cannulae prior

to dosing and at 15, 30 min and 1, 2, 4, 6, 8, 10, 12, 16, 20 and 24 hours post-dose for both i.v.

and oral routes. Additional samples at 2 and 7 min post-dose were also collected for the i.v.

doses.

Dog PK. The 2 mM AZD3783 dose solution was prepared in 10 mM lactic acid

containing 4.5% glucose. AZD3783 was administered at 1 mL/kg i.v. infusion via cephalic vein

catheter over 15 min to achieve a target dose of 2 µmol/kg. The oral dose was administered via

oral gavage at 1 mL/kg to achieve a target dose of 2 µmol/kg. Blood samples (1.2 mL) were

collected from the jugular vein prior to dosing and at 5, 15, 20, 30, 45, 75 min and 2, 3, 5, 8, 12

and 24 hours post-dose for i.v. infusion route. Pre-dose, 15, 30 min and 1, 2, 3, 5, 8, 12 and 24

hours post-dose samples were collected for orally dosed animals.

Monkey PK. The 2 mM AZD3783 dose solution was prepared with 0.3 M lactic acid in

sterile 0.9% saline. The dosing solution was adjusted to pH 6.0 using 1N sodium hydroxide.

Following filtration through a 0.22 µm filter, AZD3783 was administered in a single dose by i.v.

infusion over 15 min through a temporary percutaneous catheter placed into a peripheral vein at

1.5 mL/kg to achieve target dose of 3 µmol/kg. Blood samples (1 mL) were collected from a previously implanted chronic venous catheter prior to dosing and at 5, 15, 20, 30 min and 1, 2, 4, 6, 8, 12 and 24 hours post-dose.

   Dosing of AZD3783 in healthy male volunteers. The human PK of AZD3783 was investigated in a double-blind, placebo-controlled, randomized within each dose group, single ascending dose study in healthy male subjects. PK parameters from only the 20 mg dose group relevant to the targeted therapeutic exposure are presented here for an evaluation of PK prediction purpose. The study protocol and informed consent documents were approved by the Institutional Review Board (IRB). All subjects signed an approved written informed consent prior to any study-related activities for this clinical study. There were 8 subjects in the 20 mg dose group with 6 randomized to AZD3783 and 2 to a matching placebo. AZD3783 was administered as capsules under fasted condition. Blood samples for PK evaluation were taken between pre-dose and 72 hours post-dose. All appropriate safety components were included in the study.

   Sample processes. Rat, dog and monkey plasma samples were processed by adding 6 volumes of acetonitrile:water (8:2, v/v) containing 0.1% formic acid. After centrifugation for 15 min at 3000 rpm, the supernatants were analyzed by LC-MS. AZD3783 in human plasma samples was extracted in an Oasis HLB µ-elution 96-well plate (Waters, Milford, MA). The plate was washed with 180 µL of methanol and equilibrated in 180 µL of water before loading 150 µL of human plasma. The wells were then washed with 180 µL of 30% methanol in water and eluted with 40 µL of acetonitrile:isopropanol (1:1, v/v). A 5-µL aliquot of eluted sample was analyzed by LC-MS.

15

LC-MS analysis. For the *in vitro* samples, the separation was performed using a

Shimadzu VP HPLC system (Columbia, MD) with a Phenomenex Synergi Max-RP column (3.5

μm, 3×50 mm) coupled to a Micromass Ultima triple quadrapole mass spectrometer (Waters,

Milford, MA) under positive electrospray ionization mode. The mobile phases included 0.1%

formic acid in HPLC water (A) and 10% (v/v) methanol in acetonitrile (B). The gradient started

with 100% A for 0.3 min, was linearly increased to 95% B in 1.2 min, and held 95% B for 0.1

min before returning to 100% A. AZD3783 was quantified by integration of ion chromatogram

peak area acquired under multiple reaction monitoring (MRM) with m/z 467/235 transition.

The *in vivo* AZD3783 plasma extract was separated in a Shimadzu HPLC system with a

SepaxHP-Silica 120A analytical column (3 μm, 50×2.1 mm) coupled to a Sciex API 3000 mass

spectrometer. The isocratic eluting solvent consisted 1:10 (v/v) of 10 mM ammonium formate

(pH 4) and acetonitrile:methanol (1:1, v/v). AZD3783 and internal standard D_6-AZD3783 were

quantified by MRM under 467/235 transition for AZD3783 and 473/239 transition for

D_6-AZD3783, respectively.

Data Analysis.

In vitro 5-HT$_{1B}$ affinity and GTPγ^{35}S functional antagonist potency. Data were analyzed

by calculating IC_{50}, and K_i using the Kenakin correction for ligand depletion using following

equations.

$$B = [(K_D + L_T + R_T) - \{(K_D + L_T + R_T)^2 - 4R_TL_T\}^{1/2}] / 2 \qquad (1)$$

$$K_i = (0.5B \text{ x } IC_{50} \text{ x } K_D)/[(L_T \text{ x } R_T) + 0.5B(R_T - L_T + 0.5B - K_D)] \qquad (2)$$

where L_T and R_T are the total concentrations of the ligand and receptor, respectively. GTPγ^{35}S

functional antagonist potency was defined as antagonist concentration for 50% inhibition of the

stimulated response (EC_{50}).

Guinea pig receptor occupancy calculation. Specific binding was calculated from total

binding for each brain region by subtracting the fmol/mg values for the cerebellum (region of

non-specific receptor binding). The *in vivo* receptor occupancy for AZD3783 was indicated by a

reduction in specific binding of [*N*-methyl-^{3}H$_3$]AZ10419369 compared to vehicle controls and

represented as a percentage using equation 3:

$$\%RO = 100 \times (SB_{saline} - SB_{AZD3783})/SB_{saline} \qquad (3)$$

where %RO is percent of receptor occupancy and SB is specific binding. Treatment effects were

determined by analysis of variance (ANOVA) followed by Dunnett's post hoc test. Percent

receptor occupancy sigmoidal curves were fit and non-linear regression analysis was used to

calculate the ED_{50}, the dose that resulted in 50% receptor occupancy, and the EC_{50}, the plasma

exposure value for 50% receptor occupancy using Prism (GraphPad, San Diego CA).

Guinea pig hypothermia data. Plasma or brain EC_{50} values for reduction of agonist-

induced hypothermia were determined by non-linear regression analysis using a four parameter

Hill equation in SigmaPlot (Systat Software Inc., San Jose, CA).

Guinea pig pup vocalization data. The effects on guinea pig pup response to maternal

separation were analyzed and reported as number of calls in a 5 min period. The repeated

measures analysis of variance was conducted to assess the main effect of each drug treatment

level. Significant effects of drug treatment were followed up with Dunnett's post hoc tests to

determine which doses were significantly different from control.

Estimations of preclinical PK parameters. The PK parameters were estimated by standard non-compartmental pharmacokinetic analysis using WinNonlin version 5.2 (Pharsight, Mountain View, CA). Absolute bioavailability (%F) was determined by comparing $AUC_{0-\infty}$ values after oral to i.v. administration of AZD3783 and was expressed as F% = (AUC_{po}/AUC_{iv}) ×100%.

Extrapolation of in vivo clearance from in vitro clearance data. The drug disappearance time profile was used to assess *in vitro* intrinsic clearance CL_{int} (Houston, 1994) in microsomes ($CL_{int,m}$) and hepatocytes ($CL_{int,h}$). The *in vivo* intrinsic clearance (CL'_{int}) by liver was calculated using equation 4 or equation 5 for microsome and hepatocytes, respectively (Houston, 1994; Obach, 1999).

$$CL'_{int} = CL_{int,m} \times \frac{mg\ microsomes}{g\ liver} \times \frac{liver\ weight\ (g)}{body\ weight\ (kg)} \qquad (4)$$

$$CL'_{int} = CL_{int,h} \times \frac{million\ hepatocytes}{g\ liver} \times \frac{liver\ weight\ (g)}{body\ weight\ (kg)} \qquad (5)$$

where 45 mg microsomal protein per gram of liver tissue was applied to all species (Houston, 1994; Obach, 1997). Based on several internal study results, 1 gram of liver tissues yields approximately 200, 150, 125 and 120 million hepatocytes from human, rat, dog and cynomolgus monkey, respectively (data not shown). Calculations used 22, 40, 33 and 33 g of liver tissue per kg body weight for human, rat, dog and cynomolgus monkey, respectively. The *in vivo* hepatic clearance of AZD3783 in liver was calculated using the well stirred model as shown equation 6.

$$CL_{predict} = \frac{Q \times CL'_{int}}{Q + CL'_{int}} \qquad (6)$$

where Q is hepatic blood flow (20, 66, 38 and 44 mL/min/kg for human, rat, dog and cynomolgus monkey, respectively), CL'_{int} is the scaled intrinsic clearance determined from equation 4 or 5.

18

Extrapolation of human PK parameters from preclinical in vivo PK data. The allometric scaling of total plasma clearance (CL) and steady state volume of distribution (Vd$_{ss}$) were performed using preclinical data to fit logarithmically with linear regression to the equation 7.

$$Y = a(\text{BW})^{b} \qquad (7)$$

where Y represents CL or Vd$_{ss}$ parameters, BW is Body Weight, a and b are the coefficient and exponent of the allometric equation (Hosea et al., 2009). Human CL and Vd$_{ss}$ estimation were also performed using single species scaling from dog PK data using equations 8 and 9, respectively.

$$CL_{predict} = \left(\frac{BW_{human}}{BW_{animal}}\right)^{0.75} \times \left(CL_{animal} \times \frac{BW_{animal}}{fu_{animal}}\right) \times \left(\frac{fu_{human}}{BW_{human}}\right) \qquad (8)$$

$$Vd_{predict} = Vd_{animal} \times \frac{fu_{human}}{fu_{animal}} \qquad (9)$$

where f$_u$ is the fraction unbound in plasma. The human Vd$_{ss}$ was also calculated by applying preclinical PK data to the Oie-Tozer equation (Oie and Tozer, 1979; Obach, 1997) shown in equation 10.

$$Vd_{predict} = V_p + (fu_{human} \times V_e) + \left[(1 - fu_{human}) \times \left(\frac{R_e}{i}\right) \times V_p\right] + V_r \times \left(\frac{fu_{human}}{fu_{t(sp\ average)}}\right) \qquad (10)$$

where Vp is the human plasma volume, Ve is the extracellular fluid volume in human, Re/i is the ratio of binding proteins in extracellular fluid (except plasma) to binding proteins in plasma in human, Vr, 'remainder of the fluid', is the physical volume into which a drug can distribute minus the extracellular space in human, and fu$_t$ values for individual animals were calculated based on equation 11 (Obach, 1997).

$$fu_{t\ animal} = \frac{V_{r\ animal} \times fu_{animal}}{[Vd_{ss\ animal} - V_{p\ animal} - (fu_{animal} \times V_{e\ animal}) - [(1 - fu_{animal}) \times \left(\frac{R_{e\ animal}}{i_{animal}}\right) \times V_{p\ animal}]} \qquad (11)$$

Human PK simulation was conducted using WinNonlin 5.2 using a one compartment first order absorption and elimination model. The absorption rate constant (ka, h^{-1}) for human PK simulation was estimated from dog oral PK data.

The predicted half-life ($t_{1/2}$) in human was calculated using equation 12.

$$Predicted\ t_{1/2} = \frac{0.693 \times Vd_{predicted}}{CL_{Predicted}} \qquad (12)$$

The predicted %F in human was obtained from equation 13 based on the assumption that the fraction of AZD3783 absorbed was unity.

$$F\% = (1 - \frac{CL_{predicted}}{Q}) \times 100 \qquad (13)$$

The predicted percent receptor occupancy (%RO) was adapted from the calculation reported previously in the AZD3783 PET study (Varnäs et al., 2011).

$$\%RO = \frac{Occ_{max} \times C_{plasma}}{Ki_{plasma} + C_{plasma}} \qquad (14)$$

where Occ_{max} is the maximum receptor occupancy constrained to 100%, C_{plasma} is the total AZD3783 plasma concentration, Ki_{plasma} is the inhibition constant corresponding to AZD3783 total plasma concentration needed for half-maximum receptor occupancy (21 nM) which was from the AZD3783 PET study (Varnäs et al., 2011).

RESULTS

Pharmacology.

In vitro data. AZD3783 demonstrated strong affinity to human 5-HT$_{1B}$ receptors with a geometric mean K$_i$ of 12.5 nM (Figure 2A). AZD3783 showed similar affinity to guinea pig 5-HT$_{1B}$ receptors with K$_i$ of 11.1 nM (data not shown). In functional studies using GTPγ^{35}S binding, AZD3783 blocked 5-HT agonist induced binding of GTPγ^{35}S to human 5-HT$_{1B}$ receptors, with EC$_{50}$ of 42 nM in a 95% confidence interval of 32-56 nM and blocking efficacy above 100% (Figure 2B), consistent with an antagonist response. Schild regression analysis demonstrated a slope of unity and a K$_b$ of 1.7 nM, also consistent with reversible, competitive antagonism.

In vivo receptor occupancy of AZD3783 in the guinea pig brain. Our previous results demonstrated that [*N*-methyl-^{3}H$_3$]AZ10419369 was a selective 5HT$_{1B}$ receptor ligand (Maier et al., 2009). Pre-dose of AZD3783 reduced specific binding of [*N*-methyl-^{3}H$_3$]AZ10419369 in guinea pig brain in a dose-dependent manner (Figure 3A). Two-way ANOVA for [*N*-methyl-^{3}H$_3$]-AZ10419369 binding showed a significant main effect of AZD3783 treatment ($p < 0.001$) and brain region ($p < 0.001$). In all regions containing the 5-HT$_{1B}$ receptor (CTX, STR, MID), AZD3783 significantly inhibited specific binding with increasing dose while binding in the non-specific region, the CRB, remained unchanged . While the binding of AZD3783 was not significantly different from saline at 0.06 µmole/kg dose, AZD3783 at 0.6, 6.0 and 20 µmol/kg doses significantly blocked specific binding of the radioligand ($p < 0.05$). AZD3783 receptor occupancy was calculated from specific binding of [*N*-methyl-^{3}H$_3$]-AZ10419369 for each brain region with saline pretreatment group occupancy as the baseline. Maximal occupancy of AZD3783 was 96% in the MID, 85% in the STR and 71% in the CTX (Figure 3B). ED$_{50}$ values

21

for AZD3783 were based on occupancy values from all experimental animals (N=12): CTX

(0.27 μmol/kg), STR (0.22 μmol /kg) and MID (0.45 μmol /kg) and were representative of 50%

receptor occupancy for all target brain regions. The EC_{50} values were similar in CTX (18 nM),

STR (16 nM) and MID (18 nM). Therefore, the average EC_{50} in receptor occupancy was

estimated to be 17 nM (11 nM unbound) which was consistent to *in vitro* affinity K_i value of 12.5

nM.

Effect of AZD3783 on 5-HT$_{1B}$ agonist induced body temperature in guinea pig.

AZD3783 was shown to reverse the hypothermic effect induced by 5-HT$_{1B}$ agonist in guinea pig

(Figure 4). The EC_{50} of AZD3783 on blockade of the 5-HT$_{1B}$ agonist induced hypothermia in

guinea pig was 29 nM (18 nM unbound) and 25 nM (16 nM unbound) for plasma and brain,

respectively, and consistent with the *in vitro* K_i and receptor occupancy EC_{50} values.

Effects of AZD3783 on guinea pig pup response to maternal separation. AZD3783

significantly decreased separation-induced vocalizations (p<0.0001). The guinea pig pups

reduced vocalizations at all doses tested (p<0.01), suggesting the minimum efficacious dose was

at or below 0.2 μmol/kg (Figure 5).

Pharmacokinetic properties

Pgp efflux liability. The apparent permeability of AZD3783 in the apical to basolateral

direction in the MDCK-MDR1 cell assay was 38 nm/s at 1 μM initial concentration, suggesting

that AZD3783 would be readily permeable through blood-brain-barrier. Under the same

conditions, the flux ratio of Papp $_{B \to A}$ / Papp $_{A \to B}$ was 0.9, indicating AZD3783 was not likely a

Pgp substrate.

Plasma protein binding. The plasma protein binding of AZD3783 was determined by

equilibrium dialysis at 0.1, 1 and 10 μM and was found to be concentration independent in that

range for all species tested. The average unbound AZD3783 in plasma was 46%, 36% and 62%

for rat, dog and guinea pig, respectively. As reported by Varnäs et al. (2011) the unbound

AZD3783 in human and monkey plasma was 66% and 73%, respectively.

In vitro metabolic stability. The *in vitro* metabolic stability of AZD3783 was evaluated

using both liver microsomes and hepatocytes. The apparent CL_{int} values of AZD3783 were 15,

16, 14 and 81 μL/min/mg protein for human, rat, dog and monkey liver microsomes,

respectively. The CL_{int} values in hepatocytes were 1.6, 8.1, 7.3 and 21 μL/min/10^6 cells for

human, rat, dog and monkey, respectively. The *in vitro-in vivo* correlation (IVIVC) analysis

were performed by comparing the observed *in vivo* clearance with the predicted *in vivo*

clearance calculated from equations 4, 5 and 6 (Table 1). The predicted hepatic clearance results

for rat, dog and monkey were consistent with the observed plasma clearance from the preclinical

PK studies, indicating that phase I metabolism accounted for the majority of AZD3783

elimination in these species, and that the intrinsic clearance parameters from *in vitro* microsomal

or hepatocyte stability assay are predictive of the *in vivo* clearance.

Pharmacokinetics of AZD3783 in rats, dogs, and monkeys. The primary pharmacokinetic

parameters and the plasma profiles for AZD3783 are summarized in Table 2 and Figure 6,

respectively. The early T_{max} in preclinical species indicated a rapid absorption of AZD3783.

The elimination kinetics were monophasic in rat. There was apparent two-phase elimination in

dog and cynomolgus monkey. AZD3783 exhibited moderate plasma clearance in rat and dog

(about 29% and 45% of hepatic blood flow, respectively) with good oral bioavailability, but high

clearance in monkey (80% of hepatic blood flow). Vd_{ss} values ranged from 2.3 L/kg in rat to 5.9

L/kg in monkey (Table 2). AZD3783 also demonstrated a moderate $t_{1/2}$ of 1.4, 3.7 and 4.6 hours

in rat, dog and monkey, respectively.

23

Human Pharmacokinetics

Human pharmacokinetics prediction. Approaches applied to the estimation of human *in vivo* clearance parameter included *in vitro* scaling of clearance using equations 4, 5 and 6, multiple species allometric scaling using equation 7 and dog single species allometric scaling using equation 8 (Table 3). The predicted clearances from *in vitro* scaling (Table 1) were consistent with the observed *in vivo* plasma clearance for the preclinical species tested (Table 2) suggesting that metabolism is the major elimination pathway in these species and would also likely be in human. Multiple species allometric scaling yielded a human *in vivo* clearance of 25 mL/min/kg with exponent of 1.023 which was much greater than 0.75 (Figure 7). The single species scaling from dog resulted in a predicted human clearance of 19 mL/min/kg. It appeared from allometric or single species scaling methods that the predicted clearance would equal or exceed the human liver blood flow resulting in no bioavailability, which was inconsistent with the observed %F in rat and dog or the IVIVC predicted values in these preclinical species. Therefore, the average clearance of 6.5 mL/min/kg (0.39 L/h/kg) scaled from the human liver microsome and the hepatocyte CL_{int} was adopted as the predicted human CL value (Table 4).

The human Vd_{ss} was simulated from multiple species allometric scaling, dog single species scaling and from Oie-Tozer equation (Figure 8 and Table 3). The multiple species allometric scaling resulted in a predicted human Vd_{ss} of 7.5 L/kg with an exponent of 1.190 which was acceptably close to unity. Single species scaling from dog also yielded a similar Vd_{ss} (7.4 L/kg). Oie-Tozer equation with parameters from rat, dog and monkey predicted a human Vd_{ss} of 4.2 L/kg. A final human volume of distribution of 6.4 L/kg was adopted after averaging these results (Table 4). From the predicted CL and Vd_{ss} a half life ($t_{1/2}$) of 13 hours in human was calculated from equation 12. The predicted absorption rate constant of 3 h^{-1} was applied to

human dose prediction calculations according to the observation from the dog oral

pharmacokinetic study.

Human pharmacokinetic data. Following a 20 mg oral administration in healthy human

volunteers, AZD3783 was absorbed with a median T_{max} of 1.5 to 3.1 hours. The geometric mean

values for C_{max} and AUC were 79 nM and 1018 nM*h, respectively. The geometric mean for

clearance (CL/F) after oral administration was 0.60 L/h/kg (Table 5). The human PK parameters

obtained from this study were consistent with the human PK parameters reported by Varnäs et al.

(2011) in the AZD3783 human PET study (Table 5). The PK parameters obtained from both

human studies, dosed with 20 mg, showed values within 2 fold of the predicted human

pharmacokinetic parameters. From the 10 mg/day dose simulation (Figure 9), the predicted first

day C_{max} and plasma concentration at 24 hours were 53 and 17 nM, respectively, matching

closely with the C_{max} and plasma exposure at 24 hours observed in the human PET study at 10

mg dose (Varnäs et al., 2011).

Predicted efficacious dose in human. The predicted efficacious dose of AZD3783 in

humans was based on two sets of data, the pharmacological data from *in vitro* and *in vivo* assays

and the predicted human PK parameters. The guinea pig 5-HT$_{1B}$ receptor affinity ($K_i = 11.1$ nM)

was shown to correspond to the *in vivo* receptor occupancy unbound plasma EC_{50} value. These

binding values were also consistent with unbound plasma EC_{50} value for the blockade of 5-HT$_{1B}$

agonist induced hypothermia and the estimated minimum effective exposure value in reducing

separation-induced vocalizations in guinea pig pups. Therefore, it is anticipated that the

minimum human unbound plasma exposures (C_{min}) of AZD3783 above its K_i value of 12.5 nM

would result in efficacious effects on anxiety and depression. Multiple dose simulations using

the predicted human pharmacokinetic parameters in Table 4 indicate that a 10 mg/day dose

should achieve an estimated AZD3783 plasma C_{min} of 23 nM (14 nM unbound) and C_{max} of 75

nM (50 nM unbound) at steady state (Figure 9). Substituting simulated plasma exposure

between C_{min} and C_{max} for C_{plasma} in equation 14 resulted in a predicted 5-HT$_{1B}$ receptor

occupancy range of 52 to 78 % in human brain at steady state following 10 mg/day dosing

(Figure 9). Human PET study (Varnäs et al., 2011) showed that at 10 mg dose AZD3783

exposure around C_{max} resulted in 5-HT$_{1B}$ receptor occupancy of 61-71% in occipital cortex and

62-74% in ventral striatum, respectively, confirming the simulated receptor occupancy results.

DISCUSSION

Guinea pig was selected for this pharmacology study because of its high homology with human 5-HT$_{1B}$ receptor (Zgombick et al., 1997). This is supported by the similarity of results from the *in vitro* 5-HT$_{1B}$ receptor binding assays reported here. The *in vitro* 5-HT$_{1B}$ binding Ki value was in good agreement with guinea pig unbound plasma EC$_{50}$ values for receptor occupancy and the blockade of 5-HT$_{1B}$ agonist-induced hypothermic effect. Furthermore, the doses resulting in anxiolytic-like effects in guinea pig pups were in the same range as those showing responses in hypothermia and receptor occupancy tests. Plasma exposure correlated well with AZD3783 exposure in the brain in these studies, indicating that plasma levels could be used as a reasonable approximation of the concentration of compound in the brain. These data also showed that brain 5-HT$_{1B}$ receptor occupancy levels of 50% or higher by AZD3783 were associated with pharmacological and behavioral effects in preclinical models, consistent with the efficacious (50-87%) receptor occupancies previously reported for other GPCR antagonists (Grimwood and Hartig, 2009). A recent PET study (Varnäs et. al. 2011) showed that the average AZD3783 plasma concentrations required for 50% 5-HT$_{1B}$ receptor occupancy (K$_{i,plasma}$) in the brains of monkeys and humans were 26 and 21 nM, respectively. Based on unbound fraction of 66% for AZD3783 in human plasma, the unbound plasma concentration for AZD3783 required to achieve 50% 5-HT$_{1B}$ receptor occupancy in human brain was estimated to be 14 nM (Varnäs et. al. 2011) which also aligned with AZD3783 *in vitro* 5-HT$_{1B}$ binding *Ki* (12.5 nM) and preclinical *in vivo* pharmacology data, such as the unbound plasma EC50 values for blockade of 5-HT$_{1B}$ agonist induced hypothermia (18 nM) and brain receptor occupancy (11 nM) in guinea pig. The translation of *in vitro* binding to *in vivo* occupancy and functional potency in preclinical species and the alignment of these results with human PET K$_{i,plasma}$ values suggest

27

that 50% or greater 5-HT$_{1B}$ receptor occupancy in the brain will likely be necessary for efficacy

against symptoms of anxiety and depression in human.

The estimated absorption rate constant in human was derived directly from the observed

absorption rate constant value in dog following oral administration with the readily absorbed

aqueous formulation.   The very short T$_{max}$ indicated that absorption of AZD3783 in dog was

rapid. This could be partially the result of the readily absorbed aqueous formulation used in the

study. However, it is also possible that the physiological properties and higher pH in dog

intestine would result in more efficient absorption of the basic compound (Chiou et al., 2000;

Dressman, 1986). Therefore, the predicted human absorption rate constant may be over-

estimated compared to the observed clinical data. Previous work on AZD3783 (Zhou et al.,

2008) indicated similar metabolic pathways across species; *N*-demethylation was the major

metabolic pathway observed in hepatocyte preparations from humans, rats, dogs and guinea pigs;

CYP3A4/5 was the major primary enzyme for the metabolism of AZD3783 with lesser

contributions from CYP2C8 and CYP2D6. The extrapolated human clearance values varied

depending on the prediction method used. Allometric scaling calculations from rat, dog and

monkey yielding a predicted human clearance of 25 mL/min/kg with an exponent of 1.023, or

from dog single species scaling prediction of human clearance (19 mL/min/kg) would likely

overestimate the human clearance. The predicted *in vivo* hepatic clearances from liver

microsomes and hepatocytes scaled using the well-stirred *in vitro* scaling model were consistent

with the observed *in vivo* plasma clearance in rat, dog and monkey. Furthermore, similar

metabolic pathways between human and preclinical species also concurred that human clearance

can be predicted from human microsome or hepatocyte intrinsic clearance parameters. The

human volume of distribution predicted from multiple methods ranged from 4.2 to 7.5 L/kg.

Since there was no other confirmation process to evaluate the Vd_{ss} value obtained from these methods, the average value was adopted.

This study demonstrated that *in vitro* binding affinity and preclinical *in vivo* efficacy of AZD3783 correlated well to the level of 5-HT$_{1B}$ receptor occupancy in the brain, suggesting that like other GPCR antagonists a 50-87% receptor occupancy range in human brain would be necessary for 5-HT$_{1B}$ antagonist to show efficacious therapeutic effect. AZD3783 at 10 mg/day is expected to provide 52-78% receptor occupancy coverage at steady state and show a pharmacological effect against anxiety and depression in patients.

CONCLUSION

The preclinical pharmacodynamic and pharmacokinetic relationships reported in this study together with the clinical 5-HT$_{1B}$ receptor occupancy data reported by Varnäs and colleagues (Varnäs et al., 2011) were incorporated in our translational approach to estimate the AZD3783 dose required for antidepressant efficacy in patients. The *in vitro* 5-HT$_{1B}$ receptor affinity (Ki) of AZD3783 in guinea pig closely matched the human affinity value. The Ki values were also consistent with the guinea pig unbound plasma EC$_{50}$ level for the *in vivo* receptor occupancy and the blockade of 5-HT$_{1B}$ agonist-induced hypothermia. Doses that resulted in >50% receptor occupancy and were active in hypothermia tests also resulted in reduction of guinea pig pup separation-induced vocalizations. The predicted human 5-HT$_{1B}$ receptor occupancy of AZD3783 matched closely with the clinical receptor occupancy results. The excellent efficacy and receptor selectivity of AZD3783 combined with its favorable PK properties, and good alignment of human exposure with predictions from preclinical studies make it an excellent tool compound for further mechanistic research into the role of 5-HT$_{1B}$ receptor antagonism for the treatment of mood disorders. The approaches used in this report to develop preclinical translation model for human efficacious dose prediction could be applicable to other 5-HT$_{1B}$ antagonists.

ACKNOWLEDGEMENT

AUTHORSHIP CONTRIBUTIONS

Participated in research design: Zhang, Zhou, Maier, Widzowski, Sobotka-Briner, Brockel,

Shenvi, Bernstein and Potts and Pierson

Conducted experiments: Zhou and Sobotka-Briner.

Performed data analysis: Zhang, Zhou, Wang, Maier, Widzowski, Sobotka-Briner, Brockel,

Bernstein and Potts.

Wrote or contributed to the writing of the manuscript: Zhang, Zhou, Wang, Maier, Widzowski,

Sobotka-Briner, Brockel Shenvi, Bernstein and Pierson

REFERENCES

Ahlgren C, Eriksson A, Tellefors P, Ross SB, Stenfors C and Malmberg A (2004) In vitro characterization of AR-A000002, a novel 5-hydroxytryptamine1B autoreceptor antagonist. *Eur J Pharmacol* **499**: 67-75.

Byrne SE and Rothschild AJ (1998) Loss of antidepressant efficacy during maintenance therapy: possible mechanisms and treatments. *J Clin Psychiatry* **59**: 279-288.

Chiou WL, Jeong HY, Chung SM and Wu TC (2000) Evaluation of Using Dog as an Animal Model to Study the Fraction of Oral Dose Absorbed of 43 Drugs in Humans. *Pharm Res* **17**: 135-140.

Dawson LA, Hughes ZA, Starr KR, Storey JD, Bettelini L, Bacchi F, Arban R, Poffe A, Melotto S, Hagan JJ, et al. (2006) Characterization of the selective 5-HT$_{1B}$ receptor antagonist SB-616234-A (1-[6-(cis-3,5-dimethylpiperazin-1-yl)-2,3-dihydro-5-methoxyindol-1-yl]-1-[2'-methyl-4'-(5-methyl-1,2,4-oxadiazol-3-yl)biphenyl-4-yl]methanone hydrochloride): In vivo neurochemical and behavioural evidence of anxiolytic activity. *Neuropharmacol* **50**: 975-983.

Delgado PL, Charney DS, Price LH, Aghajanian GK, Landis H and Heninger GR (1990) Serotonin function and the mechanism of antidepressant action. Reversal of antidepressant-induced remission by rapid depletion of plasma tryptophan. *Arch Gen Psychiatry* **47**: 411-418.

Dressman JB (1986) Comparison of Canine and Human Gastrointestinal Physiology. *Pharm Res* **3**: 123-131.

Fink KB and Göthert M (2007) 5-HT receptor regulation of neurotransmitter release. *Pharmacol Rev* **59**: 360-417.

Gaster LM, Ham P, Joiner GF, King FD, Mulholland KR, Wyman PA, Hagan JJ, Price GW, Roberts C, Routledge C, Selkirk J, Slade PD and Middlemiss DN (1998) The selective 5-HT1B receptor inverse agonist SB- 224289-A, potently blocks terminal 5-HT autoreceptor function both in vitro and in vivo. *Annals N.Y. Acad Sci* **861**: 270-271.

Goldstein BJ and Goodnick PJ (1998) Selective serotonin reuptake inhibitors in the treatment of affective disorders--III. Tolerability, safety and pharmacoeconomics. *J Psychopharmacol* **12** (3 Suppl B): S55-87.

Grimwood S and Hartig PR (2009) Target site occupancy: emerging generalizations from clinical and preclinical studies. *Pharmacol Ther* **122**, 281-301.

Hagan JJ, Slade PD, Gaster L, Jeffrey P, Hatcher JP and Middlemiss DN (1977) Stimulation of 5 HT_{1B} receptors causes hypothermia in the guinea pig. *Eur J Pharmacol* **331**: 169-174.

Hetrick SE, McKensie JE, Merry SN (2010) The use of SSRIs in children and adolescents. *Current Opinion in Psychiatry* **23**:53-57.

Hillegaart V and Ahlenius S (1998) Facilitation and inhibition of male rat ejaculatory behaviour by the respective 5-HT1A and 5-HT1B receptor agonists 8-OH-DPAT and anpirtoline, as evidenced by use of the corresponding new and selective receptor antagonists NAD-299 and NAS-181. *Br J Pharmacol* **125**: 1733-1743.

Hosea NA, Collard WT, Cole S, Maurer TS, Fang RS, Jones H, Kakar SM, Nakai Y, Smith BJ, Webster R, and Beaumont K. (2009) Prediction of human pharmacokinetics from preclinical information: comparative accuracy of quantitative prediction approaches. *J Clin Pharm* **49**: 513-533.

Houston JB (1994) Utility of in vitro drug metabolism data in predicting in vivo metabolic clearance. *Biochem Pharmacol* **47**:1469-1479.

Hudzik TJ, Yanek M, Porrey T, Evenden J, Paronis C, Mastrangelo M, Ryan C, Ross S, Stenfors C (2003) Behavioral pharmacology of AR-A000002, a novel, selective 5-hydroxytryptamine$_{1B}$ antagonist. *J Pharmacol Exp Ther* **304**: 1072–1084.

Keane PE and Soubrié P (1997) Animal models of integrated serotoninergic functions: their predictive value for the clinical applicability of drugs interfering with serotoninergic transmission. In: Baumgarten HG, Göthert M (eds) *Handbook of experimental pharmacology: serotoninergic neurons and 5-HT receptors in the CNS.* Springer, Berlin Heidelberg New York, pp 707–725.

Maier DL, Sobotka-Briner C, Ding M, Powell ME, Jiang Q, Hill G, Heys JR, Elmore CS, Pierson, ME and Mrzljak L (2009) [N-methyl-^{3}H$_3$]AZ10419369 Binding to the 5-HT$_{1B}$ receptor: *in vitro* characterization and *in vivo* Receptor Occupancy. *J Pharmacol Exp Ther* **330**: 342-351.

Maj J, Chojnacka-Wójcik E, Klodzińska A, Dereń E and Moryl A (1988) Hypothermia induced by m-trifluoromethylpiperazine or m-chlorophynylpiperazine: an effect mediated by 5-HT$_{1B}$ receptors? *J Neural Transm* **73**, 43–55.

Mendlewicz J and Lecrubier Y (2000) Antidepressant selection: proceedings from a TCA/SSRI Consensus Conference. *Acta Psychiatr Scand Suppl* **403**: 5-8.

Möller HJ and Volz HP (1996) Drug treatment of depression in the 1990s. An overview of achievements and future possibilities. *Drugs* **52**: 625-638.

Moret C and Briley M (2000) The possible role of 5-HT$_{1B/D}$ receptors in psychiatric disorders and their potential as a target for therapy. *Eur J Pharmacol* **404**: 1-12.

Nabulsi N, Huang Y, Weinzimmer D, Ropchan J, Frost JJ, McCarthy T, Carson RE and Ding YS (2010) High-resolution imaging of brain 5-HT$_{1B}$ receptors in the rhesus monkey using [$_{11}$C]P943. Nucl Med Biol 37, 205-14.

Nutt DJ (2008) Relationship of neurotransmitters to the symptoms of major depressive disorder. *J Clin Psychiatry* **69** (Suppl E1): 4-7.

Obach RS (1999) Prediction of human clearance of twenty-nine drugs from hepatic microsomal intrinsic clearance data: An examination of in vitro half-life approach and nonspecific binding to microsomes. *Drug Metab Dispos* **27**: 1350-1359.

Obach RS, Baxter JG, Liston TE, Silber BM, Jones BC, MacIntyre F, Rance DJ, Wastall P (1997) The prediction of human pharmacokinetic parameters from preclinical and in vitro metabolism data. *J Pharmacol Exp Ther* **283**: 46–58.

Oie S, and TOZER TN (1979) Effect of altered plasma protein binding on apparent volume of distribution. *J Pharm Sci* **68**: 1203–1205.

Pierson ME, Andersson J, Nyberg S, McCarthy DJ, Finnema SJ, Varnäs K, Takano A, Karlsson P, Gulyás B, Medd AM, Lee CM, Powell ME, Heys JR, Potts W, Seneca N, Mrzljak L, Farde L and Halldin C (2008) [11C]AZ10419369: a selective 5-HT1B receptor radioligand suitable for positron emission tomography (PET). Characterization in the primate brain. *Neuroimage* **41**, 1075-85.

Polli JW, Wring SA, Humphreys JE, Huang L, Morgan JB, Webster LO and Serabjit-Singh CS (2001) Rational use of in vitro P-glycoprotein assays in drug discovery. *J Pharmacol Exp Ther* **299**: 620-628.

Roberts C, Price, GW and Middlemiss DN (2001) Ligands for the investigation of 5-HT autoreceptor function. *Brain Res Bull* **56**: 463-469.

Slassi A (2002) Recent Advances in 5-HT$_{1B/1D}$ receptor antagonists and agonists and their potential therapeutic applications. *Curr Topics Med Chem* **2**: 559-574.

Stenfors C, Hallerbeck T, Larsson L-G, Wallsten C, Ross SB (2004) Pharmacology of a novel selective 5-hydroxytryptamine$_{1B}$ receptor antagonist, AR-A000002. *Naunyn-Schmiedebergs Arch Pharmacol* **369**: 330–337.

Sussman N (2008) Medical Complications of SSRI and SNRI Treatment. *Primary Psychiatry* **15**: 37-41.

Tsai S-J and HONG C-J (2003) Pharmacogenetics of Selective Serotonin Reuptake Inhibitor Response in Major Depression *Current Pharmacogenomics* **1**: 1-7.

Varnäs K, Karlsson P, Nyberg S, Pierson ME, Cselényi Z, McCarthy D, Xiao A, Zhang M, Halldin C and Farde, L (2011) Dose-dependent binding of AZD3783 to brain 5-HT$_{1B}$ receptors in non-human primates and human subjects: A positron emission tomography study with [^{11}C]AZ10419369. *Psychopharmacology* **213**,533-545.

Watson JM, Burton MJ, Price GW, Jones BJ and Middlemiss DN (1996) GR127935 Acts as a partial agonist at recombinant human 5-HT$_{1D\alpha}$ and 5-HT$_{1D\beta}$ receptors. *Eur J Pharmacol* **314**: 365-372.

Zgombick JM, Bard JA, Kucharewicz SA, Urquhart DA, Weinshank RL, and Branchek TA (1997) Molecular cloning and pharmacological characterization of guinea pig 5-HT1B and 5-HT1D receptors. *Neuropharmacology* **36**: 513–524.

Zhou D, Zhang M, Otmani SA, Shen C, Wang Y and Grimm SW (2008) *In vitro* metabolism of AZ12320927: metabolite profiling in human, rat, dog, guinea pig, mouse and rabbit hepatocytes and enzymes identification in human liver microsomes. *Drug Metab Rev. Suppl* **3**, 147.

LEGENDS FOR FIGURES.

Figure 1 Chemical structure of AZD3783

Figure 2 Representative *in vitro* biding and function assay results. (A) Representative graph showing binding competition of AZD3783 with [^{3}H]-GR125743 for human 5-HT$_{1B}$ receptor. Points shown are means of duplicate determinations from a single representative experiment which was repeated for an n=18. (B) Representative graph showing inhibition of AZD3783 on 5-HT induced binding of [^{35}S]GTPγS to human 5-HT$_{1B}$ receptor. Points shown are means of triplicate determinations from a single experiment which was repeated for an n=11

Figure 3 AZD3783 receptor occupancy in guinea pig brain. (A) [*N*-methyl-^{3}H$_3$]AZ10419369 specific binding in the cortex (CTX), striatum (STR) and midbrain including the substantia nigra (MID) following pretreatment with AZD3783 at the 0.6, 6.0 and 20 μmol/kg s.c. dose (* $p<0.05$). (B) *In vivo* receptor occupancy for AZD3783 in target brain regions (CTX, STR and MID) showing the 50% occupancy range overlapped with the ED$_{50}$ dose (see text)

Figure 4 Effects of AZD3783 plasma (A) and brain (B) concentrations on 5-HT$_{1B}$ agonist induced hypothermia in guinea pigs. Veh, vehicle group

Figure 5 Effect of AZD3783 dose level on number of maternal separation-induced guinea pig pup calls

Figure 6 AZD3783 plasma concentration in rat, dog and cynomolgus monkey after i.v. and oral doses. Each point represents the mean of three determinations

Figure 7 Allometric scaling of AZD3783 clearance across animal species and humans. BW, body weight (kg); CL, clearance (mL/min)

Figure 8 Across species allometric scaling of AZD3783 volume distribution at steady state. BW, body weight (kg); Vd$_{ss}$, volume of distribution (L/kg)

Figure 9 Predicted plasma exposure (solid curve) and 5-HT$_{1B}$ receptor occupancy profile (dotted curve) of AZD3783 in human brain following 10 mg/day oral dosing. Ki is the affinity of AZD3783 for human 5-HT$_{1B}$ receptor; *fu* is unbound fraction of AZD3783 in human plasma

Table 1. Metabolic stability of AZD3783 in liver microsome and hepatocyte incubations compared to the *in vivo* Clearance

Species	Microsomes			Hepatocytes			*In vivo* PK data	
	CL_{int} (µL/min/mg protein)	Predicted $CL_{hepatic}$ (mL/min/kg)	Predicted %hepatic Blood flow	CL_{int} (µL/min/ 10^6 cells)	Predicted $CL_{hepatic}$ (mL/min/kg)	Predicted %hepatic Blood flow	CL_{Plasma} (mL/min/kg)	% hepatic blood flow
Rat	16	21	32%	8.1	28	42%	19	29%
Dog	14	14	35%	7.3	17	45%	18	45%
Monkey	81	32	73%	21	28	64%	35	80%
Human	15	7.9	38%	1.6	5.1	24%	ND	ND

ND, not determined.

Table 2. Preclinical species PK parameters

Species	Route	Dose (μmol/kg)	C_{max} (μM)	T_{max} (hr) [a]	AUC_∞ (μM*hr)	CL_{plasma} (mL/min/kg)	Vd_{ss} (L/kg)	$t_{1/2}$ (hr)	F (%)
Rat	IV	10	ND	ND	8.8±0.9	19±2.8	2.3±0.2	1.4±0.3	ND
	PO	30	9.5±3.80	0.25	26±6.0	ND	ND	ND	98
Dog	IV	2.0	ND	ND	1.9±0.1	18±0.9	4.3±0.4	3.7±0.5	ND
	PO	2.0	0.24± 0.01	1.00	1.1±0.1	ND	ND	ND	58
Monkey	IV	3.0	ND	ND	1.5±0.1	35±0.8	5.9±0.8	4.6±0.6	ND

[a] median number. ND, not determined.

Table 3. Summary of simulated human PK parameters from different scaling approaches

Prediction Method	Parameter sourcde[1]	F %	Vd_{ss} (l/kg)	CL (ml/min/kg)	$t_{1/2}$ (h)
In vitro scaling	CL Human liver microsome and hepatocyte	70	ND	6.5^2 (5.1-7.9)	ND
Allometry	CL, Vd_{ss} from rat, dog and monkey; ka from dog	0	7.5 (exponent 1.190>1.0)	25 (exponent 1.023>0.75)	3
Single SP scaling, dog	Vd_{ss}, and CL from dog	0	7.4	19	4
Single SP scaling, dog	Vd_{ss} from dog, CL from HLM/Hhep	70	7.4	6.5(5.1-7.9)	13(11-17)
Oie-Tozer Equation	Rat, dog and monkey PK parameters	ND	4.2	ND	ND

[1]Absorption rate (ka, h^{-1}) was estimated based on dog ka (3 h^{-1}); [2]CL_{int} is the average of CL_{int} from human liver microsome and human hepatocyte. ND, not determined.

42

Table 4. Summary of human PK parameters selected for dose prediction

Vd$_{ss}$ (L/kg)	CL (L/h/kg)	t$_{1/2}$ (hr)
6.4 (4.2 – 7.5)	0.39 (0.31 – 0.47)	13 (11-17)

Ka scaled from dog oral PK study 3 h^{-1}

Table 5. Comparison of simulated human PK parameters and the parameters from human subjects following 20 mg oral dose

Parameters	Predicted	Healthy male following 20mg oral dose[2]	AZD3783 Human PET study at 20mg oral dose[3]
T_{max} (hr)	1.4	2.5(1.5, 3)	2, 3, 3
$t_{1/2}$ (hr)	13	17(12, 36)	7.3, 10.7, 12.2
AUC_{0-inf} (nM*hr)	1853	1018 (224%)	761, 977, 2684
C_{max} (nM)	90	79 (21%)	54, 80, 182
C_{min} (nM)	23	ND	ND
Vd_{ss} (L/kg)	6.4	ND	ND
CL (L/h/kg)[1]	0.39	0.60 (19%)	ND

[1]CL data from clinical observation is presented as geometric mean of oral clearance, CL/F (CV%); [2]N=6, values are presented as median (min, max) value for T_{max} and $t_{1/2}$, geometric mean (CV%) for AUC and C_{max}; [3]Data were from Varnäs et al. (2011); ND, not determined.
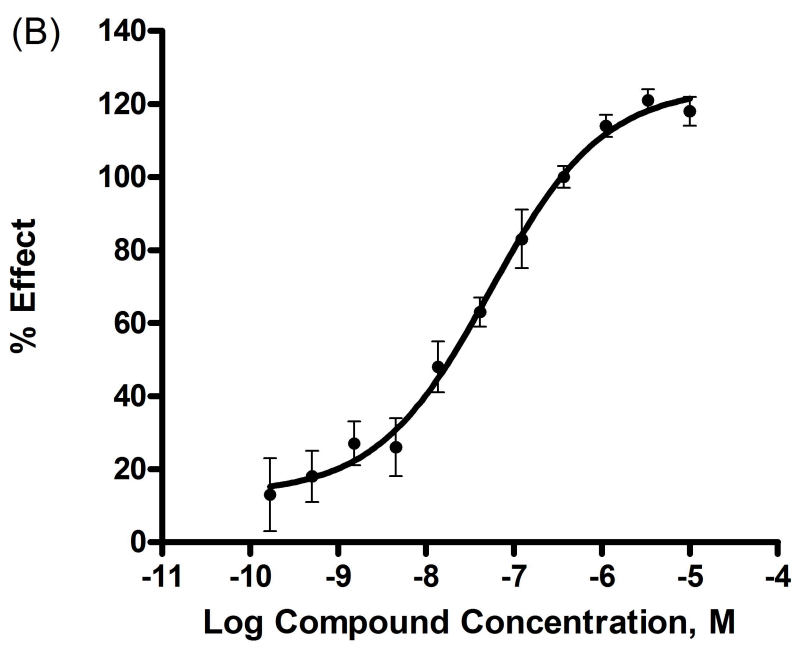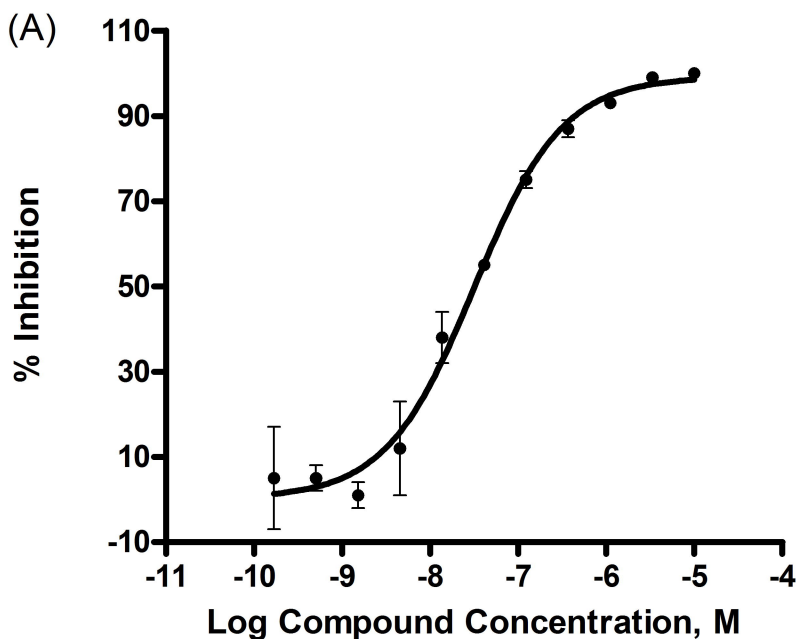
Figure 1

Figure 2

Figure 3A
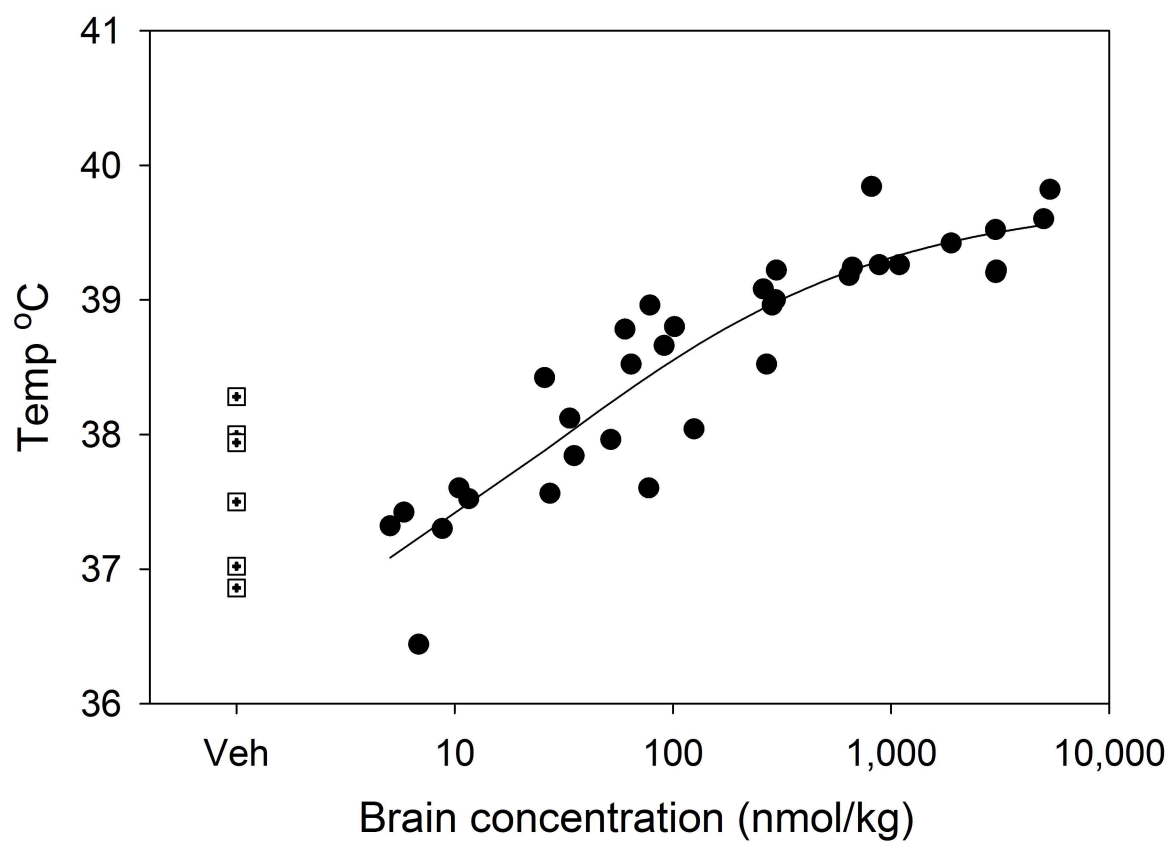

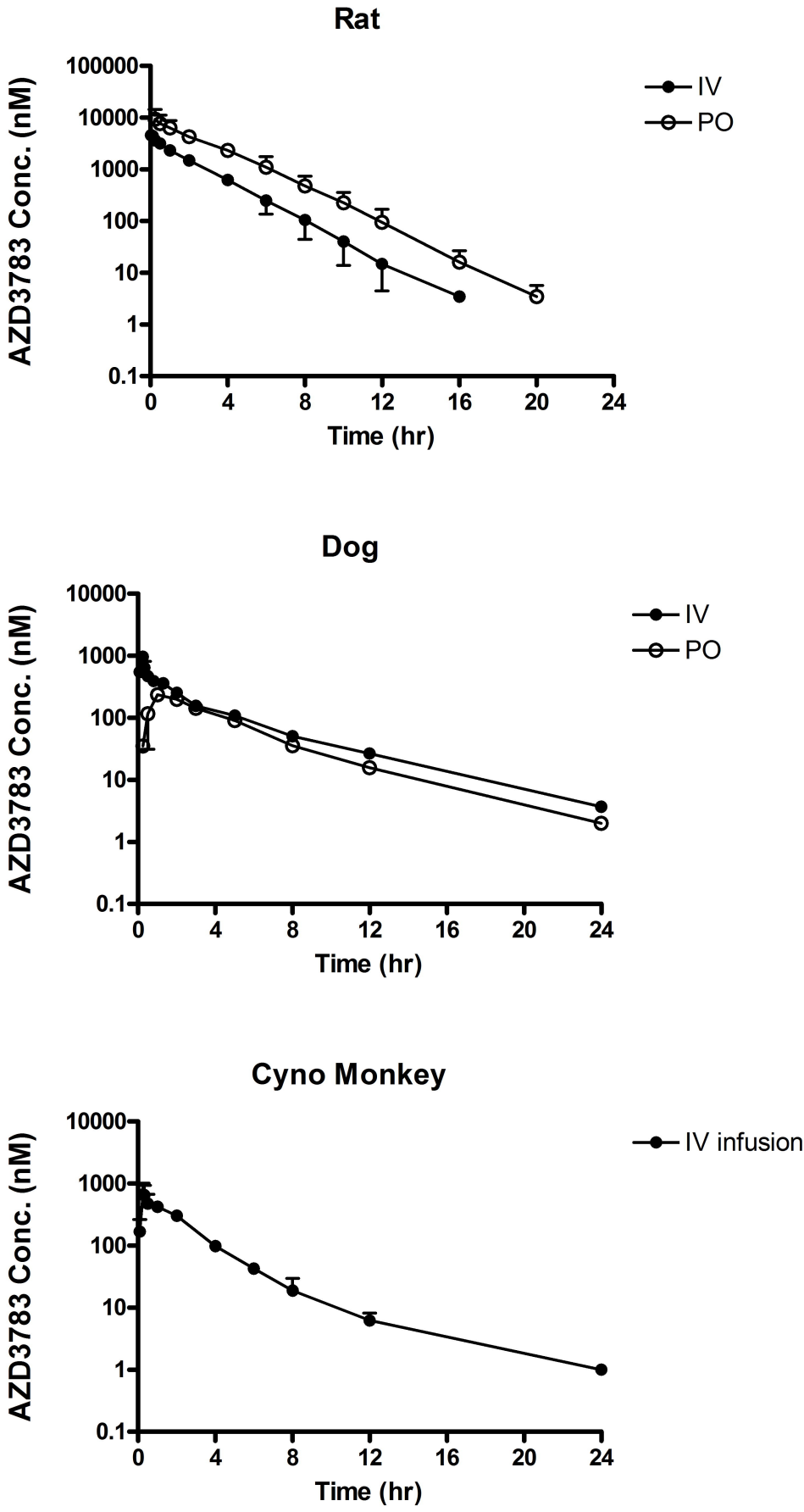# Figure 3B

Figure 4

(A)

Plasma concentration (nM)

(B)

Brain concentration (nmol/kg)
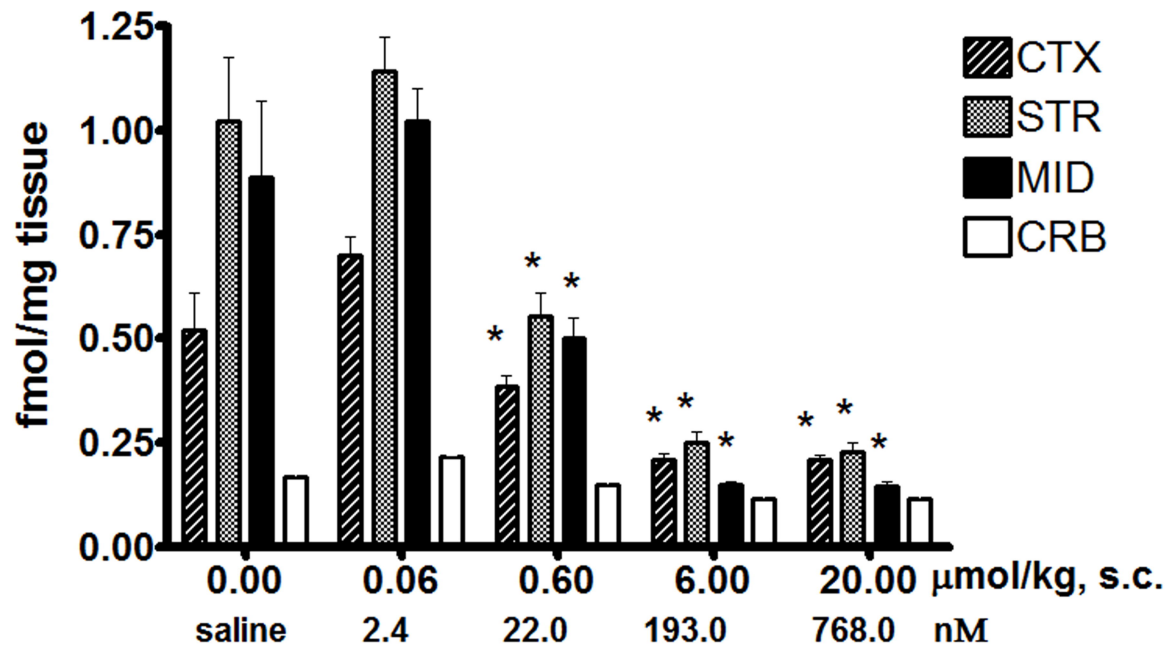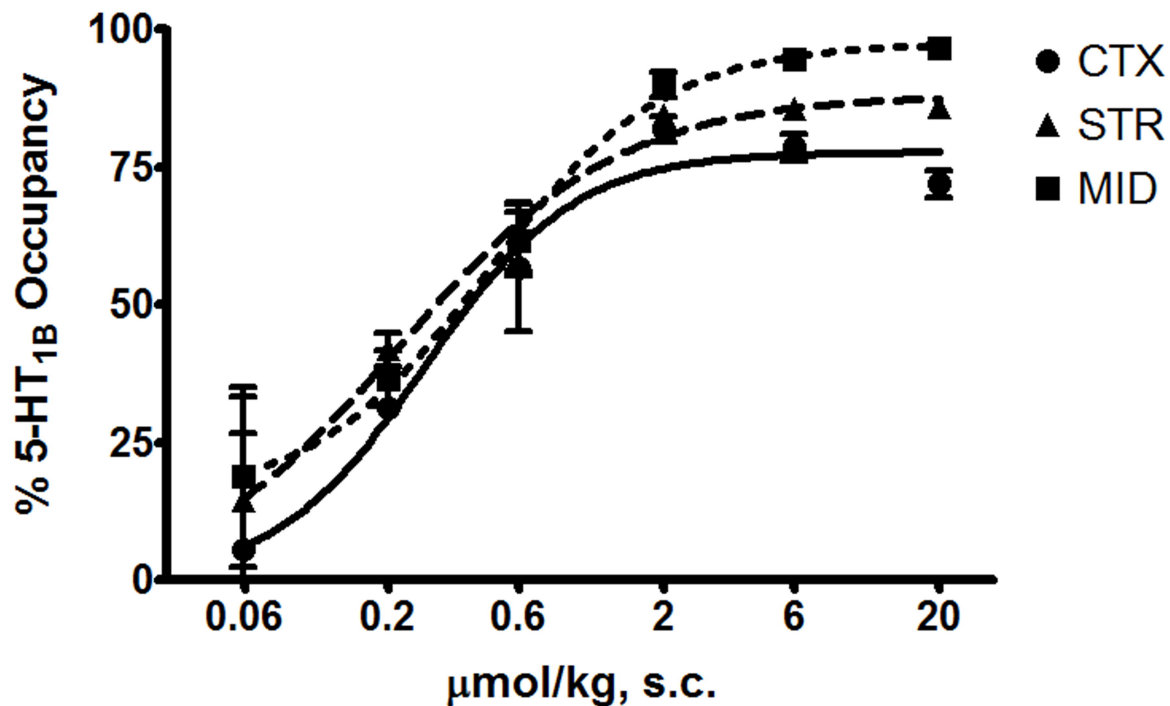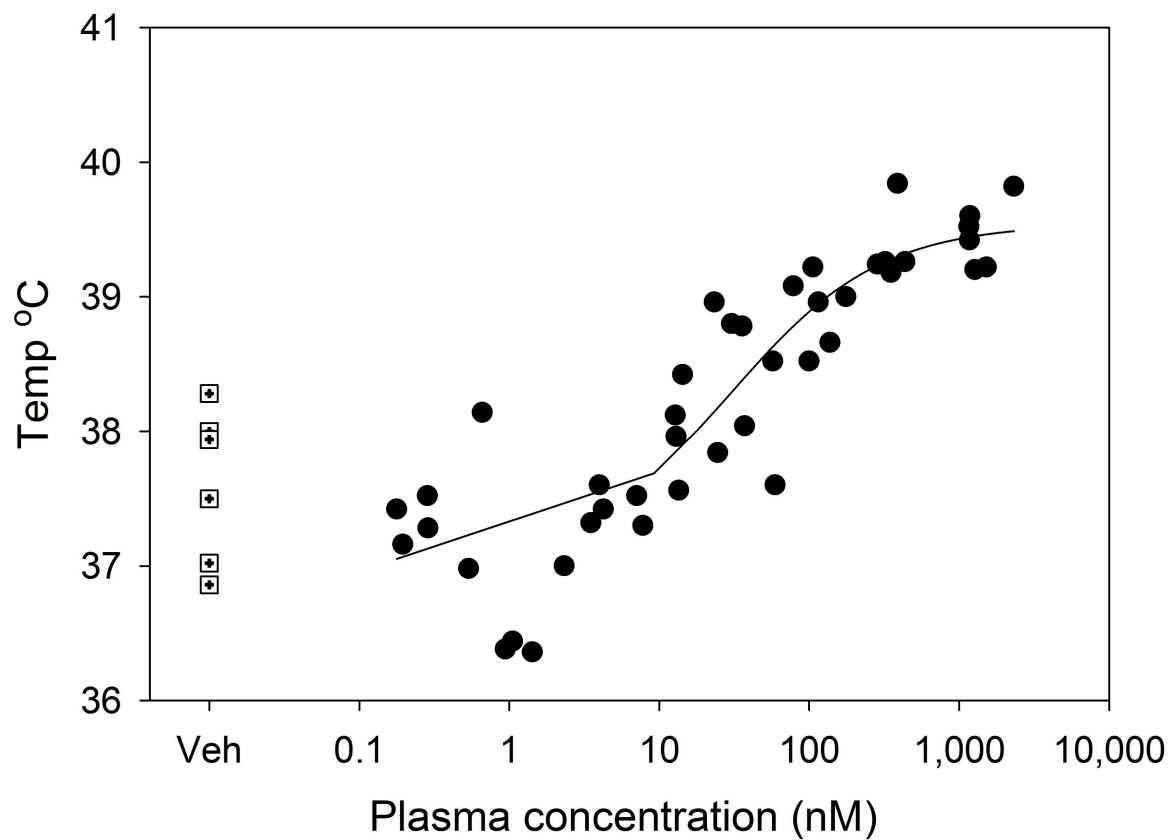
Figure 5

Figure 6

Figure 7

$y = 1.023x + 3.112$
$r^2 = 0.9850$

Figure 8

Figure 9